4

Guidance Laws for Autonomous Underwater Vehicles

Morten Breivik[1] and Thor I. Fossen[1,2]
[1]*Centre for Ships and Ocean Structures*
[2]*Department of Engineering Cybernetics*
Norwegian University of Science and Technology
Norway

1. Introduction

About 70% of the surface of the Earth is covered by oceans, and the ocean space represents a vast chamber of natural resources. In order to explore and utilize these resources, humankind depends on developing and employing underwater vehicles, not least unmanned underwater vehicles (UUVs). Today, UUVs encompass remotely operated vehicles (ROVs) and autonomous underwater vehicles (AUVs).

The first ROVs were built in the 1950s, put into commercial use in the 1980s, and are mostly used today by the offshore oil and gas industry to carry out inspection and intervention operations at subsea installations (Antonelli et al. 2008). These vehicles are teleoperated by connection to a surface vessel through an umbilical cable that provides them with power and telemetry. In particular, the dependence on a tether represents a considerable challenge for ROV deepwater operations (Whitcomb 2000).

On the other hand, AUVs are free-swimming vehicles that rely on their own energy supply. The first AUVs were built in the 1970s, put into commercial use in the 1990s, and today are mostly used for scientific, commercial, and military mapping and survey tasks (Blidberg 2001). Developed in cooperation between Kongsberg Maritime and the Norwegian Defence Research Establishment, the HUGIN series represents the most commercially successful AUV series on the world market today (Hagen et al. 2003). HUGIN vehicles have been employed for commercial applications since 1997 and for military applications since 2001. The workhorse HUGIN 3000 has an impressive 60 hours endurance at 4 knots speed with payload sensors running. Currently, the main challenges for AUVs encompass endurance, navigation, communication, and autonomy issues.

Traditionally, ROVs and AUVs have been assigned different tasks due to different strengths and weaknesses, see Fig. 1. In the future, hybrid ROV/AUV designs are expected to bridge the gap between these two main UUV types, utilizing the best of both worlds (Wernli 2000).

Regarding motion control research for UUVs, Craven et al. (1998) give an overview of modern control approaches with an emphasis on artificial intelligence techniques; Roberts & Sutton (2006) treat guidance, navigation, and control issues for unmanned marine vehicles with an emphasis on underwater vehicles; while Antonelli et al. (2008) present a state-of-the-art survey of control-related aspects for underwater robotic systems.

Source: Underwater Vehicles, Book edited by: Alexander V. Inzartsev,
ISBN 978-953-7619-49-7, pp. 582, December 2008, I-Tech, Vienna, Austria

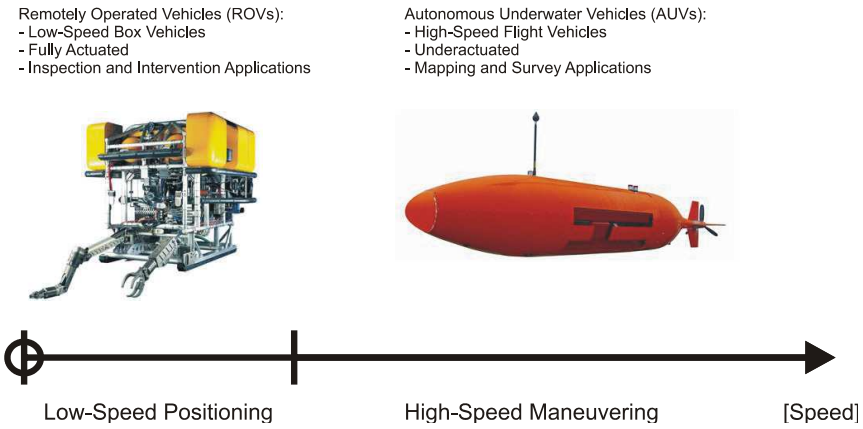

Fig. 1. The two traditional types of UUVs: ROVs and AUVs. These vehicles have different designs and perform different operations in different parts of the speed regime

An essential quality for free-swimming underwater vehicles like AUVs is their ability to maneuver accurately in the ocean space. Motion control is a fundamental enabling technology for such a quality, and every motion control system requires a guidance component. This guidance requirement serves as the main motivation for this work, whose aim is to provide a convenient overview of guidance laws applicable to motion control of AUVs. An extension of (Breivik & Fossen 2008), the exposition is deliberately kept at a basic level to make it accessible for a wide audience. Details and proofs can be found in the references.

1.1 Guidance

According to Shneydor (1998), guidance is defined as: *The process for guiding the path of an object towards a given point, which in general may be moving*. Also, the father of inertial navigation, Charles Stark Draper, states in (Draper 1971) that: *Guidance depends upon fundamental principles and involves devices that are similar for vehicles moving on land, on water, under water, in air, beyond the atmosphere within the gravitational field of earth and in space outside this field*, see Fig. 2. Thus, guidance represents a basic methodology concerned with the transient motion behavior associated with the achievement of motion control objectives.

The most rich and mature literature on guidance is probably found within the guided missile community. In one of the earliest texts on the subject (Locke 1955), a guided missile is defined as: *A space-traversing unmanned vehicle which carries within itself the means for controlling its flight path*. Today, most people would probably think about unmanned aerial vehicles (UAVs) when hearing this definition. However, guided missiles have been operational since World War II (Spearman 1978), and thus organized research on guidance theory has been conducted almost as long as organized research on control theory. The continuous progress in missile hardware and software technology has made increasingly advanced guidance concepts feasible for implementation. Today, missile guidance theory encompass a broad spectrum of guidance laws, namely: classical guidance laws; optimal guidance laws; guidance laws based on fuzzy logic and neural network theory; differential-geometric guidance laws; and guidance laws based on differential game theory.

Fig. 2. Fundamental guidance principles apply from subsea to space

As already mentioned, a classical text on missile guidance concepts is (Locke 1955), while more recent work include (Lin 1991), (Shneydor 1998), (Zarchan 2002), (Siouris 2004), and (Yanushevsky 2008). Relevant survey papers include (Pastrick et al. 1981), (Cloutier et al. 1989), (Lin & Su 2000), and (White & Tsourdos 2001). Also, very interesting personal accounts of the guided missile development during and after World War II can be found in (Haeussermann 1981), (Battin 1982), and (Fossier 1984), while MacKenzie (1990) and Westrum (1999) put the development of guided missile technology into a larger perspective.

The fundamental nature and diverse applicability of guidance principles can be further illustrated through a couple of examples. In nature, some predators are able to conceal their pursuit of prey by resorting to so-called motion camouflage techniques (Mizutani et al. 2003). They adjust their movement according to their prey so that the prey perceive them as stationary objects in the environment. These predators take advantage of the fact that some creatures detect the lateral motion component relative to the predator-prey line of sight far better than the longitudinal component. Hence, approaching predators can appear stationary to such prey by minimizing the relative lateral motion, only changing in size when closing in for the kill. Interestingly, this behavior can be directly related to the classical guidance laws from the missile literature (Justh & Krishnaprasad 2006). Also, such guidance laws have been successfully applied since the early 1990s to avoid computationally-demanding optimization methods associated with motion planning for robot manipulators operating in dynamic environments (Piccardo & Honderd 1991).

2. Motion control fundamentals

This section reviews some basic motion control concepts, including operating spaces, vehicle actuation properties, motion control scenarios, as well as the motion control hierarchy. It concludes with some preliminaries.

2.1 Operating spaces

It is useful to distinguish between different types of operating spaces when considering vehicle motion control, especially since such characterizations enable purposeful definitions of various motion control scenarios. The two most fundamental operating spaces to consider are the *work space* and the *configuration space*.

The work space, also known as the operational space (Sciavicco & Siciliano 2002), represents the physical space (environment) in which a vehicle moves. For a car, the work space is 2-dimensional (planar position), while it is 3-dimensional (spatial position) for an aircraft. Thus, the work space is a position space which is common for all vehicles of the same type.

The configuration space, also known as the joint space (Sciavicco & Siciliano 2002), is constituted by the set of variables sufficient to specify all points of a (rigid-body) vehicle in the work space (LaValle 2006). Thus, the configuration of a car is given by its planar position and orientation, while the configuration of an aircraft is given by its spatial position and attitude.

2.2 Vehicle actuation properties

Every variable associated with the configuration of a vehicle is called a degree of freedom (DOF). Hence, a car has 3 degrees of freedom, while an aircraft has 6 degrees of freedom.

The type, amount, and distribution of vehicle thrust devices and control surfaces, hereafter commonly referred to as actuators, determine the actuation property of a vehicle. We mainly distinguish between two qualitatively different actuation properties, namely *full actuation* and *underactuation*. A fully actuated vehicle is able to independently control all its DOFs simultaneously, while an underactuated vehicle is not. Thus, an underactuated vehicle is generally unable to achieve arbitrary tasks in its configuration space. However, it will be able to achieve tasks in the work space as long as it can freely project its main thrust in this space, e.g., through a combination of thrust and attitude control. In fact, this principle is the mode by which most vehicles that move through a fluid operate, from missiles to ships. Even if these vehicles had the ability to roam the work space with an arbitrary attitude, this option would represent the least energy-efficient alternative.

2.3 Motion control scenarios

In the traditional control literature, motion control scenarios are typically divided into the following categories: *point stabilization*, *trajectory tracking*, and *path following*. More recently, the concept of *maneuvering* has been added to the fold as a means to bridge the gap between trajectory tracking and path following (Skjetne et al. 2004). These scenarios are often defined by motion control objectives that are given as configuration-space tasks, which are best suited for fully actuated vehicles. Also, the scenarios typically involve desired motion that has been defined apriori in some sense. Little seems to be reported about tracking of target points for which only instantaneous motion information is available.

However, in this work, both apriori and non-apriori scenarios are considered, and all the motion control objectives are given as work-space tasks. Thus, the scenarios cover more

broadly, and are also suited for underactuated vehicles. The considered scenarios are defined in the following.

The control objective of a *target-tracking scenario* is to track the motion of a target that is either stationary (analogous to point stabilization) or that moves such that only its instantaneous motion is known, i.e., such that no information about the future target motion is available. Thus, in this case it is impossible to separate the spatio-temporal constraint associated with the target into two separate constraints.

In contrast, the control objective of a *path-following scenario* is to follow a predefined path, which only involves a spatial constraint. No restrictions are placed on the temporal propagation along the path.

However, the control objective of a *path-tracking scenario* is to track a target that moves along a predefined path (analogous to trajectory tracking). Consequently, it is possible to separate the target-related spatio-temporal constraint into two separate constraints. Still, this scenario can be viewed as a target-tracking scenario and handled with target-tracking methods, thus disregarding any apriori path information that is available.

Finally, the control objective of a *path-maneuvering scenario* is to employ knowledge about vehicle maneuverability to feasibly negotiate (or somehow optimize the negotiation of) a predefined path. As such, path maneuvering represents a subset of path following, but is less constrained than path tracking since spatial constraints always take precedence over temporal constraints. Path-maneuvering methods can also be used to handle path-tracking scenarios.

2.4 Motion control hierarchy

A vehicle motion control system can be conceptualized to involve at least three levels of control in a hierarchical structure, see Fig. 3. This figure illustrates the typical components of a marine motion control system, encompassing strategic, tactical, and execution levels of control (Valavanis et al. 1997). All the involved building blocks represent autonomy-enabling technology, but more instrumentation and additional control levels are required to attain fully autonomous operation. An example involves collision avoidance functionality, which demands additional sense and avoid components.

This work is mainly concerned with the highest (strategic) control level of Fig. 3. Termed the kinematic control level, it is responsible for prescribing vehicle velocity commands needed to achieve motion control objectives in the work space. Thus, in this work, kinematic control is equivalent to work-space control, and *kinematic controllers* are referred to as *guidance laws*. This level purely considers the geometrical aspects of motion, without reference to the forces and moments that generate such motion.

Next, the intermediate (tactical) level encompass *kinetic controllers*, which do consider how forces and moments generate vehicle motion. These controllers are typically designed by model-based methods, and must handle both parametric uncertainties and environmental disturbances. For underactuated vehicles, they must actively employ the vehicle attitude as a means to adhere to the velocities ordered by the guidance module. The intermediate control level also contains a *control allocation* block which distributes the kinetic control commands among the various vehicle actuators.

Finally, the lowest (execution) level is constituted by the individual *actuator controllers*, which ensure that the actuators behave as requested by the intermediate control module, and ultimately that the vehicle moves as prescribed by the guidance laws.

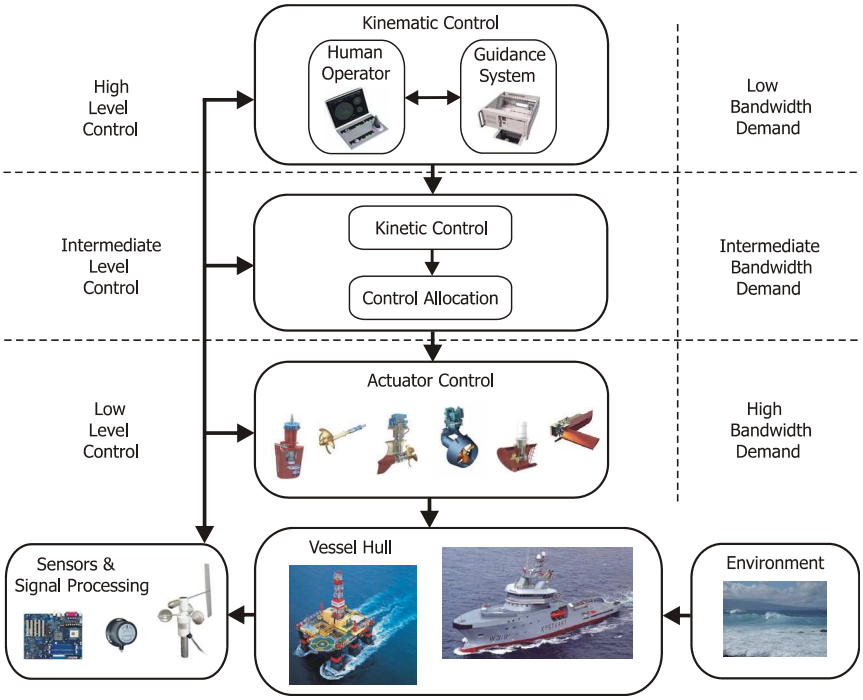

Fig. 3. The motion control hierarchy of a marine surface vessel

2.5 Preliminaries

In the missile literature, guidance laws are typically synonymous with steering laws, assuming that the speed is constant. In this work, guidance laws are either directly prescribed as velocity assignments or partitioned into separate speed and steering laws.

The guidance laws are first introduced in a 2-dimensional framework, where a kinematic vehicle is represented by its planar position $\mathbf{p}(t) \triangleq [x(t), y(t)]^{\mathrm{T}} \in \mathbb{R}^2$ and velocity $\mathbf{v}(t) \triangleq \mathrm{d}\mathbf{p}(t)/\mathrm{d}t \triangleq \dot{\mathbf{p}}(t) \in \mathbb{R}^2$, stated relative to some stationary reference frame. Since most of the AUVs of today are of the survey type, they do not need to perform spatially coupled maneuvers, but typically execute temporally separated planar maneuvers either in the horizontal plane or the vertical plane. Thus, Section 3 and 4 are relevant for such applications. Similar considerations justify the work reported in (Healey & Lienard 1993), (Caccia et al. 2000), and (Lapierre et al. 2003).

In Section 5, the planar methods are extended to a 3-dimensional framework, where a kinematic vehicle is represented by its spatial position $\mathbf{p}(t) \in \mathbb{R}^3$ and velocity $\mathbf{v}(t) \in \mathbb{R}^3$. Results on spatially coupled motion control of AUVs can be found in (Encarnação & Pascoal 2000), (Do & Pan 2003), (Aguiar & Hespanha 2004), (Breivik & Fossen 2005a), (Børhaug & Pettersen 2006), and (Refsnes et al. 2008).

Finally, note that all the illustrations of guidance principles employ the marine convention of a right-handed coordinate system whose z-axis points down.

3. Guidance laws for target tracking

In this section, guidance laws for target tracking are presented. The material is adapted from (Breivik & Fossen 2007).

Denoting the position of the target by $\mathbf{p}_t(t) \triangleq [x_t(t), y_t(t)]^T \in \mathbb{R}^2$, the control objective of a target-tracking scenario can be stated as

$$\lim_{t\to\infty} \left(\mathbf{p}(t) - \mathbf{p}_t(t) \right) = \mathbf{0}, \tag{1}$$

where $\mathbf{p}_t(t)$ is either stationary or moving by a (non-zero and bounded) velocity $\mathbf{v}_t(t) \triangleq \dot{\mathbf{p}}_t(t) \in \mathbb{R}^2$.

Concerning tracking of moving targets, the missile guidance community probably has the most comprehensive experience. They commonly refer to the object that is supposed to destroy another object as either a missile, an interceptor, or a pursuer. Conversely, the threatened object is typically called a target or an evader. Here, the designations interceptor and target will be used.

An interceptor typically undergoes 3 phases during its operation; a launch phase, a midcourse phase, and a terminal phase. The greatest accuracy demand is associated with the terminal phase, where the interceptor guidance system must compensate for the accumulated errors from the previous phases to achieve a smallest possible final miss distance to the target. Thus, 3 terminal guidance strategies will be presented in the following, namely line of sight, pure pursuit, and constant bearing. The associated geometric principles are illustrated in Fig. 4.

Note that while the main objective of a guided missile is to hit (and destroy) a physical target in finite time, we recognize the analogy of hitting (converging to) a virtual target asymptotically, i.e., the concept of asymptotic interception, as stated in (1).

3.1 Line of sight guidance

Line of sight (LOS) guidance is classified as a so-called three-point guidance scheme since it involves a (typically stationary) reference point in addition to the interceptor and the target. The LOS denotation stems from the fact that the interceptor is supposed to achieve an intercept by constraining its motion along the line of sight between the reference point and the target. LOS guidance has typically been employed for surface-to-air missiles, often mechanized by a ground station which illuminates the target with a beam that the guided missile is supposed to ride, also known as beam-rider guidance. The LOS guidance principle is illustrated in Fig. 4, where the associated velocity command is represented by a vector pointing to the left of the target.

3.2 Pure pursuit guidance

Pure pursuit (PP) guidance belongs to the so-called two-point guidance schemes, where only the interceptor and the target are considered in the engagement geometry. Simply put, the interceptor is supposed to align its velocity along the line of sight between the interceptor and the target. This strategy is equivalent to a predator chasing a prey in the animal world, and very often results in a tail chase. PP guidance has typically been employed for air-to-surface missiles. The PP guidance principle is represented in Fig. 4 by a vector pointing directly at the target.

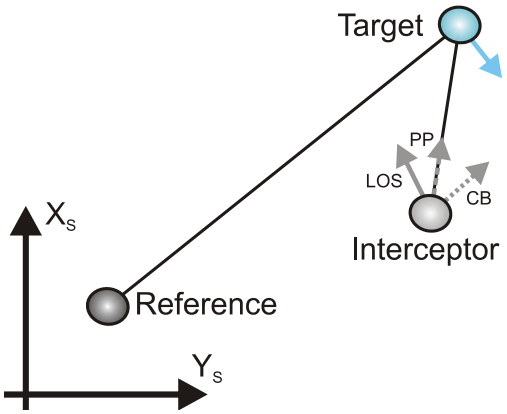

Fig. 4. The interceptor velocity commands that are associated with the classical guidance principles line of sight (LOS), pure pursuit (PP), and constant bearing (CB)

Deviated pursuit guidance is a variant of PP guidance where the velocity of the interceptor is supposed to lead the interceptor-target line of sight by a constant angle in the direction of the target movement. An equivalent term is fixed-lead navigation.

3.3 Constant bearing guidance

Constant bearing (CB) guidance is also a two-point guidance scheme, with the same engagement geometry as PP guidance. However, in a CB engagement, the interceptor is supposed to align the *relative* interceptor-target velocity along the line of sight between the interceptor and the target. This goal is equivalent to reducing the LOS rotation rate to zero such that the interceptor perceives the target at a constant bearing, closing in on a direct collision course. CB guidance is often referred to as parallel navigation, and has typically been employed for air-to-air missiles. Also, the CB rule has been used for centuries by mariners to avoid collisions at sea; steering away from a situation where another vessel approaches at a constant bearing. Thus, guidance principles can just as well be applied to avoid collisions as to achieve them. The CB guidance principle is indicated in Fig. 4 by a vector pointing to the right of the target.

The most common method of implementing CB guidance is to make the rotation rate of the interceptor velocity directly proportional to the rotation rate of the interceptor-target LOS, which is widely known as proportional navigation (PN).

CB guidance can also be implemented through the direct velocity assignment

$$\mathbf{v}(t) = \mathbf{v}_t(t) - \kappa(t)\frac{\tilde{\mathbf{p}}(t)}{|\tilde{\mathbf{p}}(t)|}, \tag{2}$$

where

$$\tilde{\mathbf{p}}(t) \triangleq \mathbf{p}(t) - \mathbf{p}_t(t) \tag{3}$$

is the line of sight vector between the interceptor and the target, $|\tilde{\mathbf{p}}(t)| \triangleq \sqrt{\tilde{\mathbf{p}}(t)^{\mathrm{T}}\tilde{\mathbf{p}}(t)} \geq 0$ is the Euclidean length of this vector, and where $\kappa(t) \geq 0$ can be chosen as

$$\kappa(t) = U_{\mathrm{a,max}} \frac{|\tilde{\mathbf{p}}(t)|}{\sqrt{\tilde{\mathbf{p}}(t)^{\mathrm{T}} \tilde{\mathbf{p}}(t) + \Delta_{\tilde{\mathrm{p}}}^2}}, \tag{4}$$

where $U_{\mathrm{a,max}} > 0$ specifies the maximum approach speed toward the target, and $\Delta_{\tilde{\mathrm{p}}} > 0$ affects the transient interceptor-target rendezvous behavior.

Note that CB guidance becomes equal to PP guidance for a stationary target, i.e., the basic difference between the two guidance schemes is whether the target velocity is used as a kinematic feedforward or not.

Returning to the example on motion camouflage, it seems that two main strategies are in use; camouflage against an object close by and camouflage against an object at infinity. The first strategy clearly corresponds to LOS guidance, while the second strategy equals CB guidance since it entails a non-rotating predator-prey line of sight.

4. Guidance laws for path scenarios

In this section, guidance laws for different path scenarios are considered, including path following, path tracking, and path maneuvering. Specifically, the guidance laws are composed of speed and steering laws, which can be combined in various ways to achieve different motion control objectives. The speed is denoted $U(t) \triangleq |\mathbf{v}(t)| = \sqrt{\dot{x}(t)^2 + \dot{y}(t)^2} \geq 0$, while the steering is denoted $\chi(t) \triangleq \mathrm{atan2}(\dot{y}(t), \dot{x}(t)) \in \mathbb{S} \triangleq [-\pi, \pi]$, where $\mathrm{atan2}(y, x)$ is the four-quadrant version of $\arctan(y/x) \in \langle -\pi/2, \pi/2 \rangle$.

Path following is ensured by proper assignments to $\chi(t)$ as long as $U(t) > 0$ since the scenario only involves a spatial constraint, while the spatio-temporal path-tracking and path-maneuvering scenarios both require explicit speed laws in addition to the steering laws. The following material is adapted from (Breivik & Fossen 2004a), (Breivik & Fossen 2005b), and (Breivik et al. 2008).

4.1 Steering laws for straight lines

Consider a straight-line path implicitly defined by two waypoints through which it passes. Denote these waypoints as $\mathbf{p}_{\mathrm{k}} \triangleq [x_{\mathrm{k}}, y_{\mathrm{k}}]^{\mathrm{T}} \in \mathbb{R}^2$ and $\mathbf{p}_{\mathrm{k+1}} \triangleq [x_{\mathrm{k+1}}, y_{\mathrm{k+1}}]^{\mathrm{T}} \in \mathbb{R}^2$, respectively. Also, consider a path-fixed reference frame with origin in $\mathbf{p}_{\mathrm{k}}$, whose x-axis has been rotated a positive angle $\alpha_{\mathrm{k}} \triangleq \mathrm{atan2}(y_{\mathrm{k+1}} - y_{\mathrm{k}}, x_{\mathrm{k+1}} - x_{\mathrm{k}}) \in \mathbb{S}$ relative to the x-axis of the stationary reference frame. Hence, the coordinates of the kinematic vehicle in the path-fixed reference frame can be computed by

$$\boldsymbol{\varepsilon}(t) = \mathbf{R}(\alpha_{\mathrm{k}})^{\mathrm{T}} (\mathbf{p}(t) - \mathbf{p}_{\mathrm{k}}), \tag{5}$$

where

$$\mathbf{R}(\alpha_{\mathrm{k}}) \triangleq \begin{bmatrix} \cos\alpha_{\mathrm{k}} & -\sin\alpha_{\mathrm{k}} \\ \sin\alpha_{\mathrm{k}} & \cos\alpha_{\mathrm{k}} \end{bmatrix}, \tag{6}$$

and $\boldsymbol{\varepsilon}(t) \triangleq [s(t), e(t)]^{\mathrm{T}} \in \mathbb{R}^2$ consists of the *along-track distance* $s(t)$ and the *cross-track error* $e(t)$, see Fig. 5. For path-following purposes, only the cross-track error is relevant since

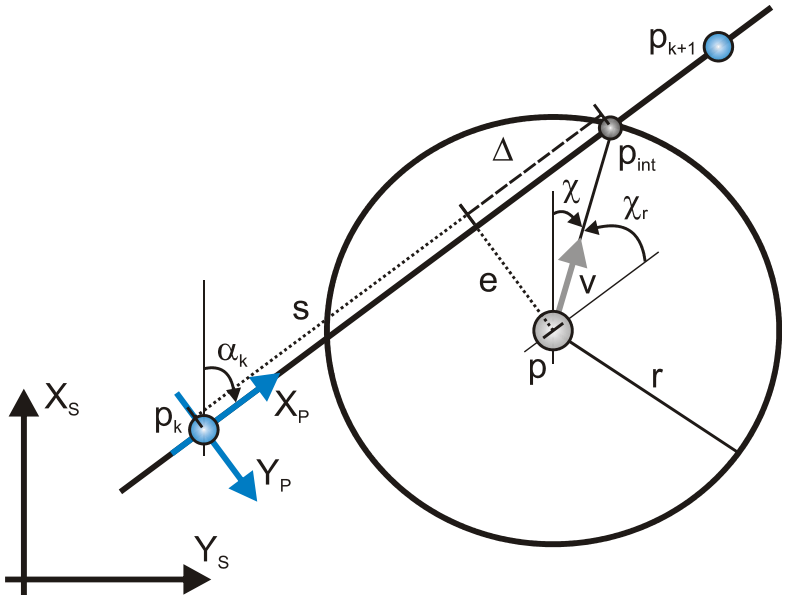

Fig. 5. The main variables associated with steering laws for straight-line paths

$e(t) = 0$ means that the vehicle has converged to the straight line. Expanding (5), the cross-track error can be explicitly stated by

$$e(t) = -(x(t) - x_k)\sin\alpha_k + (y(t) - y_k)\cos\alpha_k, \tag{7}$$

and the associated control objective for straight-line path following becomes

$$\lim_{t\to\infty} e(t) = 0. \tag{8}$$

In the following, two steering laws that ensure stabilization of $e(t)$ to the origin will be presented. The first method is used in ship motion control systems (Fossen 2002), and will be referred to as enclosure-based steering. The second method is called lookahead-based steering, and has links to the classical guidance principles from the missile literature. The two steering methods essentially operate by the same principle, but as will be made clear, the lookahead-based scheme has several advantages over the enclosure-based approach.

4.1.1 Enclosure-based steering

Imagine a circle with radius $r > 0$ enclosing $\mathbf{p}(t)$. If the circle radius is chosen sufficiently large, the circle will intersect the straight line at two points. The enclosure-based strategy for driving $e(t)$ to zero is then to direct the velocity toward the intersection point that corresponds to the desired direction of travel, which is implicitly defined by the sequence in which the waypoints are ordered. Such a solution involves directly assigning

$$\chi(t) = \text{atan2}(y_{\text{int}}(t) - y(t), x_{\text{int}}(t) - x(t)), \tag{9}$$

where $\mathbf{p}_{\text{int}}(t) \triangleq [x_{\text{int}}(t), y_{\text{int}}(t)]^{\text{T}} \in \mathbb{R}^2$ represents the intersection point of interest. In order to calculate $\mathbf{p}_{\text{int}}(t)$ (two unknowns), the following two equations must be solved

$$(x_{\text{int}}(t) - x(t))^2 + (y_{\text{int}}(t) - y(t))^2 = r^2 \tag{10}$$

$$\tan(\alpha_{\text{k}}) = \frac{y_{\text{k+1}} - y_{\text{k}}}{x_{\text{k+1}} - x_{\text{k}}}$$

$$= \frac{y_{\text{int}}(t) - y_{\text{k}}}{x_{\text{int}}(t) - x_{\text{k}}}, \tag{11}$$

where (10) represents the theorem of Pythagoras, while (11) states that the slope of the line between the two waypoints is constant. These equations are solved in the following, temporarily dropping the time dependence of the variables for notational convenience.
Denote the difference between the x- and y-position of the two waypoints as $\Delta x \triangleq x_{\text{k+1}} - x_{\text{k}}$ and $\Delta y \triangleq y_{\text{k+1}} - y_{\text{k}}$, respectively. The equations are first solved analytically assuming that $|\Delta x| > 0$ and secondly for the case $\Delta x = 0$.

Case 1: $|\Delta x| > 0$

Equation (11) results in

$$y_{\text{int}} = \left(\frac{\Delta y}{\Delta x}\right)(x_{\text{int}} - x_{\text{k}}) + y_{\text{k}} \tag{12}$$

when choosing to solve for y_{int}. For simplicity and brevity in the calculations to follow, denote

$$d \triangleq \left(\frac{\Delta y}{\Delta x}\right)$$

$$e \triangleq x_{\text{k}}$$

$$f \triangleq y_{\text{k}}.$$

Writing out (10), yields

$$x_{\text{int}}^2 - 2xx_{\text{int}} + x^2 + y_{\text{int}}^2 - 2yy_{\text{int}} + y^2 = r^2, \tag{13}$$

where

$$y_{\text{int}}^2 = \left(\left(\frac{\Delta y}{\Delta x}\right)(x_{\text{int}} - x_{\text{k}}) + y_{\text{k}}\right)^2$$

$$= (dx_{\text{int}} + (f - de))^2$$

$$= (dx_{\text{int}} + g)^2$$

$$= d^2x_{\text{int}}^2 + 2dgx_{\text{int}} + g^2, \tag{14}$$

where

$$g \triangleq f - de = y_k - \left(\frac{\Delta y}{\Delta x}\right) x_k$$

has been used. Subsequently, consider

$$2yy_{int} = 2y(dx_{int} + g) = 2dyx_{int} + 2gy, \tag{15}$$

such that (14) and (15) inserted into (13) gives

$$(1 + d^2)x_{int}^2 + 2(dg - dy - x)x_{int} + (x^2 + y^2 + g^2 - 2gy - r^2) = 0, \tag{16}$$

which is a standard, analytically-solvable second order equation. Then, denote

$$a \triangleq 1 + d^2$$

$$b \triangleq 2(dg - dy - x)$$

$$c \triangleq x^2 + y^2 + g^2 - 2gy - r^2,$$

from which the solution of (16) becomes

$$x_{int} = \frac{-b \pm \sqrt{b^2 - 4ac}}{2a}, \tag{17}$$

where if $\Delta x > 0$, then $x_{int} = \frac{-b + \sqrt{b^2 - 4ac}}{2a}$, and if $\Delta x < 0$, then $x_{int} = \frac{-b - \sqrt{b^2 - 4ac}}{2a}$. Having calculated x_{int}, y_{int} is easily obtained from (12). Note that when $\Delta y = 0$, $y_{int} = y_k$ $(= y_{k+1})$.

Case 2: $\Delta x = 0$

If $\Delta x = 0$, only equation (10) is valid, which means that

$$y_{int} = y \pm \sqrt{r^2 - (x_{int} - x)^2}, \tag{18}$$

where $x_{int} = x_k$ $(= x_{k+1})$. If $\Delta y > 0$, then $y_{int} = y + \sqrt{r^2 - (x_{int} - x)^2}$, and if $\Delta y < 0$, then $y_{int} = y - \sqrt{r^2 - (x_{int} - x)^2}$. When $\Delta x = 0$, $\Delta y = 0$ is not an option.

4.1.2 Lookahead-based steering

Here, the steering assignment is separated into two parts

$$\chi(e) = \chi_p + \chi_r(e), \tag{19}$$

where

$$\chi_p = \alpha_k \tag{20}$$

is the path-tangential angle, while

$$\chi_r(e) \triangleq \arctan\left(-\frac{e(t)}{\Delta}\right) \tag{21}$$

is a velocity-path relative angle which ensures that the velocity is directed toward a point on the path that is located a *lookahead distance* $\Delta > 0$ ahead of the direct projection of $\mathbf{p}(t)$ onto the path (Papoulias 1991), see Fig. 5.

As can be immediately noticed, this lookahead-based steering scheme is less computationally intensive than the enclosure-based approach. It is also valid for all cross-track errors, whereas the enclosure-based strategy requires $r \geq |e(t)|$. Furthermore, Fig. 5 shows that

$$e^2 + \Delta^2 = r^2, \tag{22}$$

which means that the enclosure-based approach corresponds to a lookahead-based scheme with a time-varying $\Delta(t) = \sqrt{r^2 - e(t)^2}$, varying between 0 (when $|e(t)| = r$) and r (when $|e(t)| = 0$). Only lookahead-based steering will be considered in the following.

4.2 Piecewise linear paths

If a path is made up of n straight-line segments connected by n+1 waypoints, a strategy must be employed to purposefully switch between these segments as they are traversed. In (Fossen 2002), it is suggested to associate a so-called circle of acceptance with each waypoint, with radius $R_{k+1} > 0$ for waypoint $k+1$, such that the corresponding switching criterion becomes

$$(x_{k+1} - x(t))^2 + (y_{k+1} - y(t))^2 \leq R_{k+1}^2, \tag{23}$$

i.e., to switch when $\mathbf{p}(t)$ has entered the waypoint-enclosing circle. Note that for the enclosure-based approach, such a switching criterion entails the additional (conservative) requirement $r \geq R_{k+1}$.

A perhaps more suitable switching criterion solely involves the along-track distance $s(t)$, such that if the total along-track distance between waypoints $\mathbf{p}_k$ and $\mathbf{p}_{k+1}$ is denoted s_{k+1}, a switch is made when

$$(s_{k+1} - s(t)) \leq R_{k+1}, \tag{24}$$

which is similar to (23), but has the advantage that $\mathbf{p}(t)$ does not need to enter the waypoint-enclosing circle for a switch to occur, i.e., no restrictions are put on the cross-track error. Thus, if no intrinsic value is associated with visiting the waypoints, and their only purpose is to implicitly define a piecewise linear path, there is no reason to apply the circle-of-acceptance switching criterion (23).

4.3 Steering for circles

Denote the center of a circle with radius $r_c > 0$ as $\mathbf{p}_c \triangleq [x_c, y_c]^T \in \mathbb{R}^2$. Subsequently, consider a path-fixed reference frame with origin at the direct projection of $\mathbf{p}(t)$ onto the circular

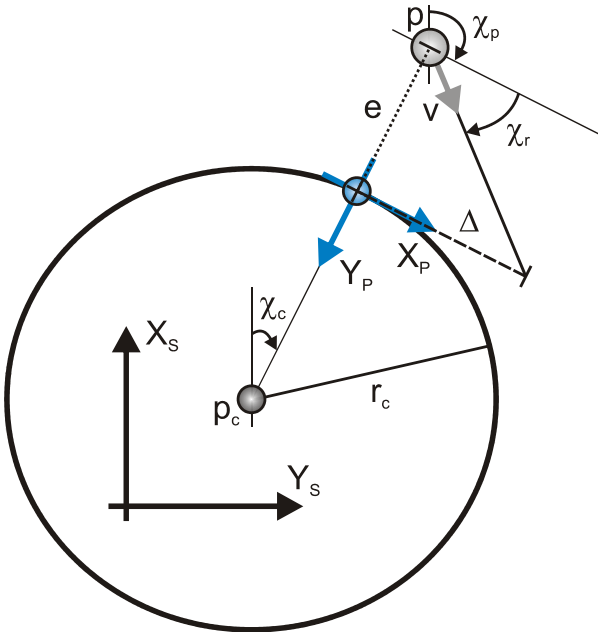

Fig. 6. The main variables associated with steering for circles

path, see Fig. 6. The x-axis of this reference frame has been rotated a positive angle (relative to the x-axis of the stationary reference frame)

$$\chi_{\mathrm{p}}(t) = \chi_{\mathrm{c}}(t) + \lambda\frac{\pi}{2}, \tag{25}$$

where

$$\chi_{\mathrm{c}}(t) \triangleq \operatorname{atan2}\big(y(t) - y_{\mathrm{c}}, x(t) - x_{\mathrm{c}}\big), \tag{26}$$

and $\lambda \in \{-1,1\}$ with $\lambda = -1$ corresponding to anti-clockwise motion and $\lambda = 1$ to clockwise motion. Hence, χ_{p} becomes time-varying for circular (curved) motion, as opposed to the constant χ_{p} associated with straight lines (20). Also, note that (26) is undefined for $\mathbf{p}(t) = \mathbf{p}_{\mathrm{c}}$, i.e., when the kinematic vehicle is located at the circle center. In this case, any projection of $\mathbf{p}(t)$ onto the circular path is valid, but in practice this problem can be alleviated by, e.g., purposefully choosing $\chi_{\mathrm{c}}(t)$ based on the motion of $\mathbf{p}(t)$.

Since the path-following control objective for circles is identical to (8), lookahead-based steering can be employed, implemented by using (19) with (25) instead of (20), and

$$\begin{aligned} e(t) &= r_{\mathrm{c}} - \left|\mathbf{p}(t) - \mathbf{p}_{\mathrm{c}}\right| \\ &= r_{\mathrm{c}} - \sqrt{(x(t) - x_{\mathrm{c}})^2 - (y(t) - y_{\mathrm{c}})^2} \end{aligned} \tag{27}$$

in (21), see Fig. 6. Note that the lookahead distance Δ is no longer defined along the path, but (in general) along the x-axis of the path-fixed frame (i.e., along the path tangential associated with the origin of the path-fixed frame). An along-track distance $s(t)$ can also be computed relative to some fixed point on the circle perimeter if required.

4.4 Steering for regularly parameterized paths

Consider a planar path continuously parameterized by a scalar variable $\varpi \in \mathbb{R}$, such that the position of a point belonging to the path is represented by $\mathbf{p}_{\mathrm{p}}(\varpi) \in \mathbb{R}^2$. Thus, the path is a one-dimensional manifold that can be expressed by the set

$$\mathcal{P} \triangleq \left\{ \mathbf{p} \in \mathbb{R}^2 \mid \mathbf{p} = \mathbf{p}_{\mathrm{p}}(\varpi) \ \forall \ \varpi \in \mathbb{R} \right\}. \tag{28}$$

Regularly parameterized paths belong to the subset of $\mathcal{P}$ for which $\left| \mathbf{p}_{\mathrm{p}}'(\varpi) \right| \triangleq \left| \mathrm{d}\mathbf{p}_{\mathrm{p}}(\varpi) / \mathrm{d}\varpi \right|$ is non-zero and finite, which means that such paths never degenerate into a point nor have corners. These paths include both straight lines (zero curvature) and circles (constant curvature). However, most are paths with varying curvature. For such paths, it is not trivial to calculate the cross-track error $e(t)$ required in (21).

Although it is possible to calculate the exact projection of $\mathbf{p}(t)$ onto the path by applying the so-called Serret-Frenet equations, such an approach suffers from a kinematic singularity associated with the osculating circle of the instantaneous projection point (Samson 1992). For every point along a curved path, there exists an associated tangent circle with radius $r(\varpi) = 1 / c(\varpi)$, where $c(\varpi)$ is the curvature at the path point. This circle is known as the osculating circle, and if at any time $\mathbf{p}(t)$ is located at the origin of the osculating circle, the projected point on the path will have to move infinitely fast, which is not possible. This kinematic singularity effect necessitates a different approach to obtain the cross-track error required for steering purposes. The solution considered here seems to first have been suggested in (Aicardi et al. 1995), then refined and put into a differential-geometric framework in (Lapierre et al. 2003), and finally extended into the form presented below in (Breivik & Fossen 2004b).

Thus, consider an arbitrary path point $\mathbf{p}_{\mathrm{p}}(\varpi)$. Subsequently, consider a path-fixed reference frame with origin at $\mathbf{p}_{\mathrm{p}}(\varpi)$, whose x-axis has been rotated a positive angle (relative to the x-axis of the stationary reference frame)

$$\chi_{\mathrm{p}}(\varpi) = \operatorname{atan2}\left(y_{\mathrm{p}}'(\varpi), x_{\mathrm{p}}'(\varpi) \right), \tag{29}$$

such that

$$\boldsymbol{\varepsilon}(t) = \mathbf{R}(\chi_{\mathrm{p}})^{\mathrm{T}} (\mathbf{p}(t) - \mathbf{p}_{\mathrm{p}}(\varpi)), \tag{30}$$

where $\boldsymbol{\varepsilon}(t) = \left[s(t), e(t) \right]^{\mathrm{T}} \in \mathbb{R}^2$ represents the *along-track* and *cross-track errors* relative to $\mathbf{p}_{\mathrm{p}}(\varpi)$, decomposed in the path-fixed reference frame by

$$\mathbf{R}(\chi_{\mathrm{p}}) = \begin{bmatrix} \cos\chi_{\mathrm{p}} & -\sin\chi_{\mathrm{p}} \\ \sin\chi_{\mathrm{p}} & \cos\chi_{\mathrm{p}} \end{bmatrix}. \tag{31}$$

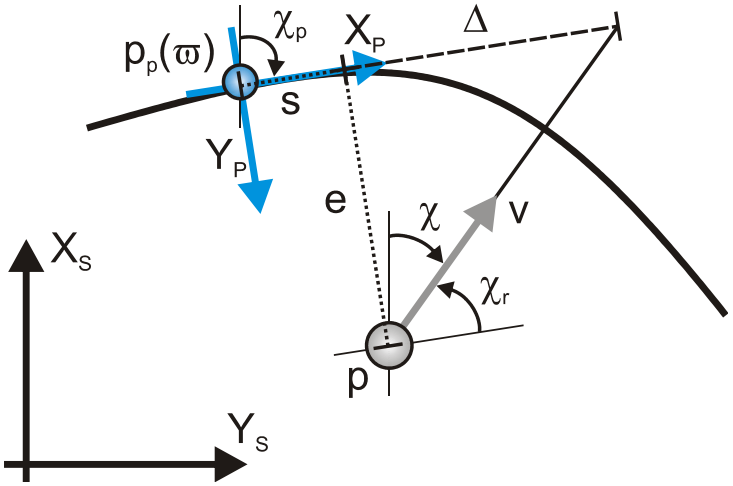

Fig. 7. The main variables associated with steering for regularly parameterized paths

In contrast to (8), the path-following control objective now becomes

$$\lim_{t\to\infty} \boldsymbol{\varepsilon}(t) = \mathbf{0}, \tag{32}$$

and in order to reduce $\boldsymbol{\varepsilon}(t)$ to zero, $\mathbf{p}(t)$ and $\mathbf{p}_{\mathrm{p}}(\varpi)$ can collaborate with each other. Specifically, $\mathbf{p}_{\mathrm{p}}(\varpi)$ can contribute by moving toward the direct projection of $\mathbf{p}(t)$ onto the x-axis of the path-fixed reference frame by assigning

$$\dot{\varpi} = \frac{U(t)\cos\chi_{\mathrm{r}}(e) + \gamma s(t)}{\left|\mathbf{p}_{\mathrm{p}}'(\varpi)\right|}, \tag{33}$$

where $\chi_{\mathrm{r}}(e)$ is given by (21), $\gamma > 0$, and $\left|\mathbf{p}_{\mathrm{p}}'(\varpi)\right| = \sqrt{x_{\mathrm{p}}'(\varpi)^2 + y_{\mathrm{p}}'(\varpi)^2}$. As can be seen, the first element of the numerator represents a kinematic feedforward of the projected speed of $\mathbf{p}(t)$ onto the path tangential, while the second element represents a linear feedback term whose purpose is to reduce the along-track error to zero. Hence, the path-constrained attractor $\mathbf{p}_{\mathrm{p}}(\varpi)$ tracks the motion of $\mathbf{p}(t)$, which steers by the location of $\mathbf{p}_{\mathrm{p}}(\varpi)$ through the cross-track error of (30) by employing (19) with (29) and (21) for $U(t) > 0$. Such an approach suffers from no kinematic singularities, and ensures that $\boldsymbol{\varepsilon}(t)$ is reduced to zero for regularly parameterized paths. To avoid initial transients in $e(t)$, the initial along-track error $s(0)$ can be minimized offline.

4.4.1 Relations to classical guidance laws

Drawing a connection to the classical guidance principles of the missile literature, lookahead-based steering can be interpreted as pure pursuit of the lookahead point. Convergence to $\mathbf{p}_{\mathrm{p}}(\varpi)$ is thus achieved as $\mathbf{p}(t)$ in vain chases a carrot located a distance Δ further ahead along the path tangential. However, in (Papoulias 1992), the lookahead point is suggested to be placed further ahead along the path instead of along the path tangential,

which leads to a steady-state offset in the cross-track error for curved paths. In this case, the velocity of $\mathbf{p}(t)$ cannot be aligned with the velocity of $\mathbf{p}_{\mathrm{p}}(\varpi)$ for zero cross-track error. This distinction is vital for curved paths, but not for straight-line paths, where the path tangential is always directed along the path. Thus, in general, the pursued carrot must be located along the path tangential and not along the path itself. Nevertheless, the along-path approach has been widely reported in the literature, see, e.g., (Ollero & Heredia 1995), (Rankin et al. 1997), and (Castaño et al. 2005).

4.4.2 Off-path traversing of curved paths

In some applications, it can be desirable to perform off-path traversing of regularly parameterized paths. Specifically, off-path traversing of curved paths requires the use of two virtual points to avoid kinematic singularities. This concept was originally suggested in (Breivik et al. 2006), and used for formation control of ships in (Breivik et al. 2008).

4.4.3 Path parameterizations

Although the recently-presented guidance method also can be applied for both straight lines and circles, the analytic, path-specific approaches presented previously are often preferable since they do not require numerical integrations such as (33). However, for completeness, applicable (arc-length) parameterizations of straight lines and circles are given in the following.

Parameterization of straight lines

A planar straight line can be parameterized by $\varpi \in \mathbb{R}$ as

$$x_{\mathrm{p}}(\varpi) = x_{\mathrm{f}} + \varpi \cos\alpha \tag{34}$$

$$y_{\mathrm{p}}(\varpi) = y_{\mathrm{f}} + \varpi \sin\alpha, \tag{35}$$

where $\mathbf{p}_{\mathrm{f}} \triangleq [x_{\mathrm{f}}, y_{\mathrm{f}}]^{\mathrm{T}} \in \mathbb{R}^2$ represents a fixed point on the path (for which ϖ is defined relative to), and $\alpha \in \mathbb{S}$ represents the orientation of the path relative to the x-axis of the stationary reference frame (corresponding to the direction of increasing ϖ).

Parameterization of circles

A planar circle can be parameterized by $\varpi \in \mathbb{R}$ as

$$x_{\mathrm{p}}(\varpi) = x_{\mathrm{c}} + r_{\mathrm{c}} \cos\left(\frac{\varpi}{r_{\mathrm{c}}}\right) \tag{36}$$

$$y_{\mathrm{p}}(\varpi) = y_{\mathrm{c}} + \lambda r_{\mathrm{c}} \sin\left(\frac{\varpi}{r_{\mathrm{c}}}\right), \tag{37}$$

where $\mathbf{p}_{\mathrm{c}} = [x_{\mathrm{c}}, y_{\mathrm{c}}]^{\mathrm{T}} \in \mathbb{R}^2$ represents the circle center, $r_{\mathrm{c}} > 0$ represents the circle radius, and $\lambda \in \{-1, 1\}$ decides in which direction $\mathbf{p}_{\mathrm{p}}(\varpi)$ traces the circumference; $\lambda = -1$ for anti-clockwise motion and $\lambda = 1$ for clockwise motion.

4.5 Speed law for path tracking

As previously stated, the control objective of a path-tracking scenario is to track a target that is constrained to move along a path. Denoting the path-parameterization variable associated with the path-traversing target by $\varpi_t(t) \in \mathbb{R}$, the control objective is identical to (1) with $\mathbf{p}_t(t) = \mathbf{p}_p(\varpi_t(t))$. Here, $\varpi_t(t)$ can be updated by

$$\dot{\varpi}_t = \frac{U_t(t)}{\left|\mathbf{p}_p'(\varpi_t)\right|}, \tag{38}$$

which means that the target point traverses the path with the speed profile $U_t(t) > 0$, which can also be made to vary with ϖ_t.

Naturally, this problem can be solved by the target-tracking methods of Section 3, e.g., through the direct velocity assignment (2). However, by using such methods, all available path information is disregarded, and $\mathbf{p}(t)$ will appear to be "cutting corners" in its pursuit of $\mathbf{p}_p(\varpi_t(t))$, seeing only $\mathbf{p}_t(t)$.

Another approach is to employ the path knowledge that is apriori available, to divide the path-tracking problem into two tasks, i.e., a spatial task and a temporal task (Skjetne et al. 2004). The spatial task was just solved in the previous part, while the temporal task can be solved by employing the speed law

$$U(t) = \left|\mathbf{p}_p'(\varpi)\right| \left(\frac{U_t(t)}{\left|\mathbf{p}_p'(\varpi_t)\right|} - \mu \frac{\tilde{\varpi}(t)}{\sqrt{\tilde{\varpi}(t)^2 + \Delta_{\tilde{\varpi}}^2}} \right), \tag{39}$$

where

$$\tilde{\varpi}(t) \triangleq \varpi(t) - \varpi_t(t), \tag{40}$$

μ can be chosen as

$$\mu = \rho \frac{U_t(t)}{\left|\mathbf{p}_p'(\varpi_t)\right|}, \ \rho \in \langle 0, 1], \tag{41}$$

and where $\Delta_{\tilde{\varpi}} > 0$ specifies the rendezvous behavior toward the target, such that

$$U(t) = U_t(t) \left(1 - \rho \frac{\tilde{\varpi}(t)}{\sqrt{\tilde{\varpi}(t)^2 + \Delta_{\tilde{\varpi}}^2}} \right) \frac{\left|\mathbf{p}_p'(\varpi(t))\right|}{\left|\mathbf{p}_p'(\varpi_t(t))\right|}, \tag{42}$$

which means that the kinematic vehicle speeds up to catch the target when located behind it, and speeds down to wait when located in front of it. Hence, this approach entails a synchronization-law extension of the path-following scenario, where no corners are cut.

4.6 Path maneuvering aspects

The path-maneuvering scenario involves the use of knowledge about vehicle maneuverability constraints to design purposeful speed and steering laws that allow for feasible path negotiation. Since this work only deals with kinematic considerations, such

deliberations are outside of its scope. However, relevant work in this vein include (Sheridan 1966), (Yoshimoto et al. 2000), (Skjetne et al. 2004), (Børhaug et al. 2006), (Subbotin et al. 2006), (Gomes et al. 2006), and (Sharp 2007). Much work still remains to be done on this topic, which represents a rich source of interesting and challenging problems.

4.7 Steering laws as saturated control laws

Rewriting (21) as

$$\chi_{\mathrm{r}}(e) = \arctan\left(-k_{\mathrm{p}} e(t)\right),\ k_{\mathrm{p}} = \frac{1}{\Delta} > 0, \tag{43}$$

it can be seen that the lookahead-based steering law is equivalent to a saturated proportional control law, effectively mapping $e \in \mathbb{R}$ into $\chi_{\mathrm{r}}(e) \in \langle -\pi/2, \pi/2 \rangle$.

As can be inferred from the geometry of Fig. 5, a small lookahead distance implies aggressive steering, which intuitively is confirmed by a correspondingly large proportional gain in the saturated control interpretation. This interpretation also suggests the possibility of introducing, e.g., integral action into the steering law, such that

$$\chi_{\mathrm{r}}(e) = \arctan\left(-k_{\mathrm{p}} e(t) - k_{\mathrm{i}} \int_0^t e(\tau)\mathrm{d}\tau\right), \tag{44}$$

where $k_{\mathrm{i}} > 0$ represents the integral gain. Note that such integral action is not necessary in a purely kinematic setting, but can be particularly useful for underactuated AUVs that can only steer by attitude information, enabling them to follow straight-line paths while under the influence of constant ocean currents even without having access to velocity information. Thus, considering horizontal path following along straight lines, the desired yaw angle can be computed by

$$\psi_{\mathrm{d}}(e) = \alpha_{\mathrm{k}} + \chi_{\mathrm{r}}(e) \tag{45}$$

with $\chi_{\mathrm{r}}(e)$ as in (44). In practice, to avoid overshoot and windup effects, care must be taken when using integral action in the steering law. Specifically, the integral term should only be used when a steady-state off-track condition has been detected.

For those AUVs that do have access to velocity information, temporal integration can be replaced by spatial integration in order to minimize overshoot and windup problems (Davidson et al. 2002), employing

$$\chi_{\mathrm{r}}(e) = \arctan\left(-k_{\mathrm{p}} e(t) - k_{\mathrm{i}} \int_0^s e(\sigma)\mathrm{d}\sigma\right), \tag{46}$$

where for straight-line paths

$$\int_0^s e(\sigma)\mathrm{d}\sigma = \int_0^t e(\tau)\frac{\mathrm{d}\sigma}{\mathrm{d}\tau}\mathrm{d}\tau \tag{47}$$

$$= \int_0^t e(\tau) U(\tau) \cos(\chi(\tau) - \alpha_{\mathrm{k}})\mathrm{d}\tau, \tag{48}$$

which means that integration only occurs when the velocity has a component along the path. Also, derivative action can be added to the steering law in order to obtain a damped transient response toward the path.

5. Guidance laws for 3D scenarios

In this section, guidance laws for 3D motion control scenarios are considered. For spatial target-tracking purposes, the guidance principles of Section 3 remain equally valid, and the velocity assignment (2) is directly applicable for 3D target tracking. However, the steering laws of Section 4 need to be extended. Specifically, in what follows, lookahead-based steering will be put into a spatial framework for regularly parameterized paths, adapted from (Breivik & Fossen 2005b). Note that the path-tracking speed law (42) need not be modified, and can be directly applied to 3D scenarios.

Now, represent the kinematic vehicle by its spatial position $\mathbf{p}(t) \triangleq \left[x(t), y(t), z(t)\right]^{\mathrm{T}} \in \mathbb{R}^3$ and velocity $\mathbf{v}(t) \triangleq \dot{\mathbf{p}}(t) \in \mathbb{R}^3$, stated relative to some stationary reference frame. Also, the speed is represented by $U(t) \triangleq \left|\mathbf{v}(t)\right| = \sqrt{\dot{x}(t)^2 + \dot{y}(t)^2 + \dot{z}(t)^2} \geq 0$, while the steering is characterized by the two angular variables $\chi(t) \triangleq \operatorname{atan2}\left(\dot{y}(t), \dot{x}(t)\right) \in \mathbb{S}$ (the azimuth angle) and $\upsilon(t) \triangleq \operatorname{atan2}\left(-\dot{z}(t), \sqrt{\dot{x}(t)^2 + \dot{y}(t)^2}\right) \in \mathbb{S}$ (the elevation angle). Path following is then ensured by proper assignments to $\chi(t)$ and $\upsilon(t)$ as long as $U(t) > 0$.

Then, consider a spatial path continuously parameterized by a scalar variable $\varpi \in \mathbb{R}$, such that the position of a point belonging to the path is represented by $\mathbf{p}_{\mathrm{p}}(\varpi) \in \mathbb{R}^3$. Thus, the path can be expressed by the set

$$\mathcal{P} \triangleq \left\{ \mathbf{p} \in \mathbb{R}^3 \,|\, \mathbf{p} = \mathbf{p}_{\mathrm{p}}(\varpi) \;\forall\; \varpi \in \mathbb{R} \right\}. \tag{49}$$

Subsequently, consider an arbitrary path point $\mathbf{p}_{\mathrm{p}}(\varpi)$, and define a path-fixed reference frame with origin at this point. Starting with the same orientation as the stationary frame, two consecutive elementary rotations can be performed to arrive at this path-fixed frame. The first is to positively rotate the stationary frame an angle

$$\chi_{\mathrm{p}}(\varpi) = \operatorname{atan2}\left(y_{\mathrm{p}}'(\varpi), x_{\mathrm{p}}'(\varpi)\right) \tag{50}$$

about its z-axis, while the second is to positively rotate the resulting intermediate frame an angle

$$\upsilon_{\mathrm{p}}(\varpi) = \operatorname{atan2}\left(-z_{\mathrm{p}}'(\varpi), \sqrt{x_{\mathrm{p}}'(\varpi)^2 + y_{\mathrm{p}}'(\varpi)^2}\right) \tag{51}$$

about its y-axis. These rotations can also be represented by the rotation matrices

$$\mathbf{R}(\chi_{\mathrm{p}}) \triangleq \begin{bmatrix} \cos\chi_{\mathrm{p}} & -\sin\chi_{\mathrm{p}} & 0 \\ \sin\chi_{\mathrm{p}} & \cos\chi_{\mathrm{p}} & 0 \\ 0 & 0 & 1 \end{bmatrix} \tag{52}$$

and

$$\mathbf{R}(\upsilon_{\mathrm{p}}) \triangleq \begin{bmatrix} \cos\upsilon_{\mathrm{p}} & 0 & \sin\upsilon_{\mathrm{p}} \\ 0 & 1 & 0 \\ -\sin\upsilon_{\mathrm{p}} & 0 & \cos\upsilon_{\mathrm{p}} \end{bmatrix}, \tag{53}$$

respectively. Hence, the full rotation can be represented by

$$\mathbf{R}(\chi_{\mathrm{p}}, \upsilon_{\mathrm{p}}) \triangleq \mathbf{R}(\chi_{\mathrm{p}})\mathbf{R}(\upsilon_{\mathrm{p}}), \tag{54}$$

such that

$$\boldsymbol{\varepsilon}(t) = \mathbf{R}(\chi_{\mathrm{p}}, \upsilon_{\mathrm{p}})^{\mathrm{T}}(\mathbf{p}(t) - \mathbf{p}_{\mathrm{p}}(\varpi)), \tag{55}$$

where $\boldsymbol{\varepsilon}(t) = [s(t), e(t), h(t)]^{\mathrm{T}} \in \mathbb{R}^3$ represents the *along-track*, *cross-track*, and *vertical-track errors* relative to $\mathbf{p}_{\mathrm{p}}(\varpi)$, decomposed in the path-fixed reference frame. The path-following control objective is identical to (32), and $\boldsymbol{\varepsilon}(t)$ can be reduced to zero by assigning an appropriate steering law to the velocity of $\mathbf{p}(t)$ as well as a purposeful collaborative behavior to $\mathbf{p}_{\mathrm{p}}(\varpi)$.

Specifically, the steering law involves

$$\chi_{\mathrm{r}}(e) \triangleq \arctan\left(-\frac{e(t)}{\Delta}\right), \tag{56}$$

which is equivalent to (21) with $\Delta > 0$, used to shape the convergence behavior toward the xz-plane of the path-fixed frame, and

$$\upsilon_{\mathrm{r}}(h) \triangleq \arctan\left(\frac{h(t)}{\sqrt{e(t)^2 + \Delta^2}}\right), \tag{57}$$

used to shape the convergence behavior toward the xy-plane of the path-fixed frame, see Fig. 8. Also, $\mathbf{p}_{\mathrm{p}}(\varpi)$ moves collaboratively toward the direct projection of $\mathbf{p}(t)$ onto the x-axis of the path-fixed reference frame by

$$\dot{\varpi} = \frac{U(t)\cos\chi_{\mathrm{r}}(e)\cos\upsilon_{\mathrm{r}}(h) + \gamma s(t)}{\left|\mathbf{p}_{\mathrm{p}}'(\varpi)\right|}, \tag{58}$$

where $\gamma > 0$ and $\left|\mathbf{p}_{\mathrm{p}}'(\varpi)\right| = \sqrt{x_{\mathrm{p}}'(\varpi)^2 + y_{\mathrm{p}}'(\varpi)^2 + z_{\mathrm{p}}'(\varpi)^2}$. In sum, four angular variables (50), (51), (56), and (57) are used to specify the 3D steering law required for path-following purposes. Fortunately, these variables can be compactly represented by the azimuth angle

$$\chi(\chi_{\mathrm{p}}, \upsilon_{\mathrm{p}}, \chi_{\mathrm{r}}, \upsilon_{\mathrm{r}}) = \operatorname{atan2}\left(f(\chi_{\mathrm{p}}, \upsilon_{\mathrm{p}}, \chi_{\mathrm{r}}, \upsilon_{\mathrm{r}}), g(\chi_{\mathrm{p}}, \upsilon_{\mathrm{p}}, \chi_{\mathrm{r}}, \upsilon_{\mathrm{r}})\right), \tag{59}$$

where

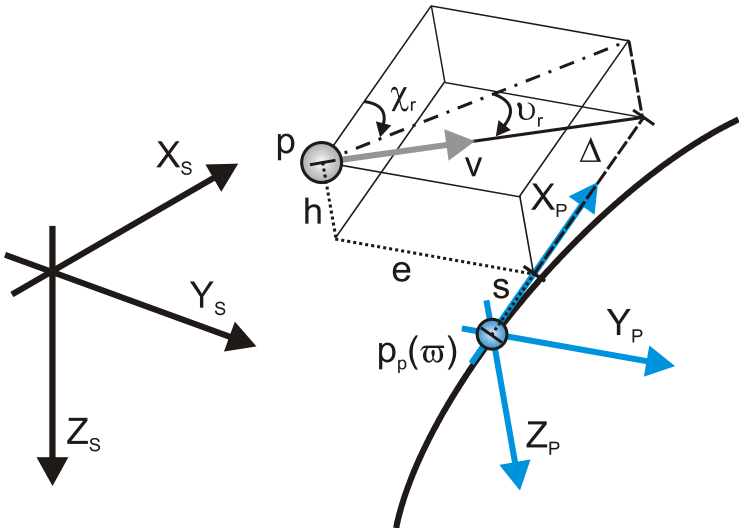

Fig. 8. The main variables associated with steering for regularly parameterized 3D paths

$$f(\chi_p,\upsilon_p,\chi_r,\upsilon_r) = \cos\chi_p \sin\chi_r \cos\upsilon_r - \sin\chi_p \sin\upsilon_p \sin\upsilon_r + \sin\chi_p \cos\upsilon_p \cos\chi_r \cos\upsilon_r \tag{60}$$

and

$$g(\chi_p,\upsilon_p,\chi_r,\upsilon_r) = -\sin\chi_p \sin\chi_r \cos\upsilon_r - \cos\chi_p \sin\upsilon_p \sin\upsilon_r + \cos\chi_p \cos\upsilon_p \cos\chi_r \cos\upsilon_r, \tag{61}$$

and the elevation angle

$$\upsilon(\upsilon_p,\chi_r,\upsilon_r) = \arcsin(\sin\upsilon_p \cos\chi_r \cos\upsilon_r + \cos\upsilon_p \sin\upsilon_r). \tag{62}$$

Through the use of trigonometric addition formulas, it can be shown that (59) is equivalent to (19) in the 2D case, i.e., when $\upsilon_p = \upsilon_r = 0$.

5.1 Path parameterizations

Applicable (arc-length) parameterizations of straight lines and helices are now given.

5.1.1 Parameterization of straight lines

A spatial straight line can be parameterized by $\varpi \in \mathbb{R}$ as

$$x_p(\varpi) = x_f + \varpi \cos\alpha \cos\beta \tag{63}$$

$$y_p(\varpi) = y_f + \varpi \sin\alpha \cos\beta \tag{64}$$

$$z_p(\varpi) = z_f - \varpi \sin\beta, \tag{65}$$

where $\mathbf{p}_f \triangleq [x_f, y_f, z_f]^T \in \mathbb{R}^3$ represents a fixed point on the path (for which ϖ is defined relative to), and $\alpha \in \mathbb{S}$ represents the azimuth angle of the path, while $\beta \in \mathbb{S}$ represents the elevation angle of the path (both corresponding to the direction of increasing ϖ).

5.1.2 Parameterization of helices

A helix can be parameterized by $\varpi \in \mathbb{R}$ as

$$x_p(\varpi) = x_c + r_c \cos\left(\frac{\varpi}{\sqrt{2}r_c}\right) \tag{66}$$

$$y_p(\varpi) = y_c + \lambda r_c \sin\left(\frac{\varpi}{\sqrt{2}r_c}\right) \tag{67}$$

$$z_p(\varpi) = z_c - \frac{\varpi}{\sqrt{2}}, \tag{68}$$

where $\mathbf{p}_c = [x_c, y_c, z_c]^T \in \mathbb{R}^3$ represents the origin of the helix center (for which ϖ is defined relative to), $r_c > 0$ represents the radius of the horizontally-projected circle of the helix, and $\lambda \in \{-1, 1\}$ decides in which direction this horizontally-projected circle is traced; $\lambda = -1$ for anti-clockwise motion and $\lambda = 1$ for clockwise motion. Here, an increase in ϖ corresponds to movement in the negative direction of the z-axis of the stationary frame.

6. Conclusions

This work has given an overview of guidance laws applicable to motion control of AUVs in 2D and 3D. Specifically, considered scenarios have included target tracking, where only instantaneous information about the target motion is available, as well as path scenarios, where spatial information is available apriori. For target-tracking purposes, classical guidance laws from the missile literature were reviewed, in particular line of sight, pure pursuit, and constant bearing. For the path scenarios, enclosure-based and lookahead-based guidance laws were presented. Relations between the guidance laws have been discussed, as well as interpretations toward saturated control.

7. References

Aguiar, A. P. & Hespanha, J. P. (2004). Logic-based switching control for trajectory-tracking and path-following of underactuated autonomous vehicles with parametric modeling uncertainty. In: *Proceedings of the ACC'04, Boston, Massachusetts, USA*

Aicardi, M.; Casalino, G.; Bicchi, A. & Balestrino, A. (1995). Closed loop steering of unicycle-like vehicles via Lyapunov techniques. *IEEE Robotics and Automation Magazine* 2(1), 27—35

Antonelli, G.; Fossen, T. I. & Yoerger, D. R. (2008). Underwater robotics. In: *Springer Handbook of Robotics* (B. Siciliano and O. Khatib, Eds.). pp. 987— 1008. Springer-Verlag Berlin Heidelberg

Battin, R. H. (1982). Space guidance evolution - A personal narrative. *Journal of Guidance, Control, and Dynamics* 5(2), 97—110

Blidberg, D. R. (2001). The development of autonomous underwater vehicles (AUVs); a brief summary. In: *Proceedings of the ICRA'01, Seoul, Korea*

Breivik, M. & Fossen, T. I. (2004a). Path following of straight lines and circles for marine surface vessels. In: *Proceedings of the 6th IFAC CAMS, Ancona, Italy*

Breivik, M. & Fossen, T. I. (2004b). Path following for marine surface vessels. In: *Proceedings of the OTO'04, Kobe, Japan*

Breivik, M. & Fossen, T. I. (2005a). Guidance-based path following for autonomous underwater vehicles. In: *Proceedings of the OCEANS'05, Washington D.C., USA*

Breivik, M. & Fossen, T. I. (2005b). Principles of guidance-based path following in 2D and 3D. In: *Proceedings of the CDC-ECC'05, Seville, Spain*

Breivik, M.; Subbotin, M. V. & Fossen, T. I. (2006). Kinematic aspects of guided formation control in 2D. In: *Group Coordination and Cooperative Control* (K. Y. Pettersen, J. T. Gravdahl and H. Nijmeijer, Eds.). pp. 54—74. Springer-Verlag Heidelberg

Breivik, M. & Fossen, T. I. (2007). Applying missile guidance concepts to motion control of marine craft. In: *Proceedings of the 7th IFAC CAMS, Bol, Croatia*

Breivik, M.; Hovstein, V. E. & Fossen, T. I. (2008). Ship formation control: A guided

leader-follower approach. In: *Proceedings of the 17th IFAC World Congress, Seoul, Korea*

Breivik, M. & Fossen, T. I. (2008). Guidance laws for planar motion control. In: *Proceedings of the CDC'08, Cancun, Mexico*

Børhaug, E. & Pettersen, K. Y. (2006). LOS path following for underactuated underwater vehicle. In: *Proceedings of the 7th IFAC MCMC, Lisbon, Portugal*

Børhaug, E.; Pettersen, K. Y. & Pavlov, A. (2006). An optimal guidance scheme for cross-track control of underactuated underwater vehicles. In: *Proceedings of the MED'06, Ancona, Italy*

Caccia, M.; Bruzzone, G. & Veruggio, G. (2000). Guidance of unmanned underwater vehicles: Experimental results. In: *Proceedings of the ICRA'00, San Francisco, California, USA*

Castaño, A. R.; Ollero, A.; Vinagre, B. M. & Chen, Y. Q. (2005). Synthesis of a spatial lookahead path tracking controller. In: *Proceedings of the 16th IFAC World Congress, Prague, Czech Republic*

Cloutier, J. R.; Evers, J. H. & Feeley, J. J. (1989). Assessment of air-to-air missile guidance and control technology. *IEEE Control Systems Magazine* 9(6), 27—34

Craven, P. J.; Sutton, R. & Burns, R. S. (1998). Control strategies for unmanned underwater vehicles. *Journal of Navigation* 51, 79—105

Davidson, M.; Bahl, V. & Moore, K. L. (2002). Spatial integration for a nonlinear path tracking control law. In: *Proceedings of the ACC'02, Anchorage, Alaska, USA*

Do, K. D. & Pan, J. (2003). Robust and adaptive path following for underactuated autonomous underwater vehicles. In: *Proceedings of the ACC'03, Denver, Colorado, USA*

Draper, C. S. (1971). Guidance is forever. *Navigation* 18(1), 26—50

Encarnação, P. & Pascoal, A. (2000). 3D path following for autonomous underwater vehicle. In: *Proceedings of the CDC'00, Sydney, Australia*

Fossen, T. I. (2002). *Marine Control Systems: Guidance, Navigation and Control of Ships, Rigs and Underwater Vehicles*. Marine Cybernetics

Fossier, M. W. (1984). The development of radar homing missiles. *Journal of Guidance, Control, and Dynamics* 7(6), 641—651

Gomes, P.; Silvestre, C.; Pascoal, A. & Cunha, R. (2006). A path-following controller for the DELFIMx autonomous surface craft. In: *Proceedings of the 7th IFAC MCMC, Lisbon, Portugal*

Haeussermann, W. (1981). Developments in the field of automatic guidance and control of rockets. *Journal of Guidance and Control* 4(3), 225—239

Hagen, P. E.; Størkersen, N. J. & Vestgård, K. (2003). The HUGIN AUVs – Multi-role capability for challenging underwater survey operations. *EEZ International*

Healey, A. J. & Lienard, D. (1993). Multivariable sliding-mode control for autonomous diving and steering of unmanned underwater vehicles. *IEEE Journal of Oceanic Engineering* 18(3), 327—339

Justh, E. W. & Krishnaprasad, P. S. (2006). Steering laws for motion camouflage. *Proceedings of the Royal Society A* 462(2076), 3629—3643

Lapierre, L.; Soetanto, D. & Pascoal, A. (2003). Nonlinear path following with applications to the control of autonomous underwater vehicles. In: *Proceedings of the CDC'03, Maui, Hawaii, USA*

LaValle, S. M. (2006). *Planning Algorithms*. Cambridge University Press

Lin, C.-F. (1991). *Modern Navigation, Guidance, and Control Processing, Volume II*. Prentice Hall, Inc.

Lin, C.-L. & Su, H.-W. (2000). Intelligent control theory in guidance and control system design: An overview. *Proceedings of the National Science Council, ROC* 24(1), 15—30

Locke, A. S. (1955). *Guidance*. D. Van Nostrand Company, Inc.

MacKenzie, D. A. (1990). *Inventing Accuracy: A Historical Sociology of Nuclear Missile Guidance*. MIT Press

Mizutani, A.; Chahl, J. S. & Srinivasan, M. V. (2003). Motion camouflage in dragonflies. *Nature* 423, 604

Ollero, A. & Heredia, G. (1995). Stability analysis of mobile robot path tracking. In: *Proceedings of the IROS'95, Pittsburgh, Pennsylvania, USA*

Papoulias, F. A. (1991). Bifurcation analysis of line of sight vehicle guidance using sliding modes. *International Journal of Bifurcation and Chaos* 1(4), 849—865

Papoulias, F. A. (1992). Guidance and control laws for vehicle pathkeeping along curved trajectories. *Applied Ocean Research* 14(5), 291—302

Pastrick, H. L.; Seltzer, S. M. & Warren, M. E. (1981). Guidance laws for short-range tactical missiles. *Journal of Guidance and Control* 4(2), 98—108

Piccardo, H. R. & Honderd, G. (1991). A new approach to on-line path planning and generation for robots in non-static environments. *Robotics and Autonomous Systems* 8(3), 187—201

Rankin, A. L.; Crane III, C. D. & Armstrong II, D. G. (1997). Evaluating a PID, pure pursuit, and weighted steering controller for an autonomous land vehicle. In: *Proceedings of the SPIE Mobile Robotics XII, Pittsburgh, Pennsylvania, USA*

Refsnes, J. E.; Sørensen, A. J. & Pettersen, K. Y. (2008). Model-based output feedback control of slender-body underactuated AUVs: Theory and experiments. *IEEE Transactions on Control Systems Technology* 16(5), 930—946

Roberts, G. N. & Sutton, R. (2006). *Advances in Unmanned Marine Vehicles*. The Institution of Electrical Engineers

Samson, C. (1992). Path following and time-varying feedback stabilization of a wheeled mobile robot. In: *Proceedings of the ICARCV'92, Singapore*

Sciavicco, L. & Siciliano, B. (2002). *Modelling and Control of Robot Manipulators*. Springer-Verlag London Ltd.

Sharp, R. S. (2007). Application of optimal preview control to speed-tracking of road vehicles. *Proceedings of the Institution of Mechanical Engineers, Part C: Journal of Mechanical Engineering Science* 221(12), 1571—1578

Sheridan, T. B. (1966). Three models of preview control. *IEEE Transactions on Human Factors in Electronics* 7(2), 91—102

Shneydor, N. A. (1998). *Missile Guidance and Pursuit: Kinematics, Dynamics and Control*. Horwood Publishing Ltd.

Siouris, G. M. (2004). *Missile Guidance and Control Systems*. Springer-Verlag New York, Inc.

Skjetne, R.; Fossen, T. I. & Kokotović, P. V. (2004). Robust output maneuvering for a class of nonlinear systems. *Automatica* 40(3), 373—383

Spearman, M. L. (1978). Historical development of worldwide guided missiles. In: *AIAA 16th Aerospace Sciences Meeting, Huntsville, Alabama, USA*

Subbotin, M. V.; Dăcić, D. B. & Smith, R. S. (2006). Preview based path-following in the presence of input constraints. In: *Proceedings of the ACC'06, Minneapolis, Minnesota, USA*

Valavanis, K. P.; Gracanin, D.; Matijasevic, M.; Kolluru, R. & Demetriou, G. A. (1997). Control architectures for autonomous underwater vehicles. *IEEE Control Systems Magazine* 17(6), 48—64

Wernli, R. L. (2000). AUV commercialization – Who's leading the pack?. In: *Proceedings of the OCEANS'00, Providence, Rhode Island, USA*

Westrum, R. (1999). *Sidewinder: Creative Missile Development at China Lake*. Naval Institute Press

Whitcomb, L. (2000). Underwater robotics: Out of the research laboratory and into the field. In: *Proceedings of the ICRA'00, San Francisco, California, USA*

White, B. A. & Tsourdos, A. (2001). Modern missile guidance design: An overview. In: *Proceedings of the IFAC Automatic Control in Aerospace, Bologna, Italy*

Yanushevsky, R. (2008). *Modern Missile Guidance*. CRC Press

Yoshimoto, K.; Katoh, M. & Inoue, K. (2000). A vision-based speed control algorithm for autonomous driving. In: *Proceedings of the AVEC'00, Ann Arbor, Michigan, USA*

Zarchan, P. (2002). *Tactical and Strategic Missile Guidance*. 4th ed.. American Institute of Aeronautics and Astronautics, Inc.

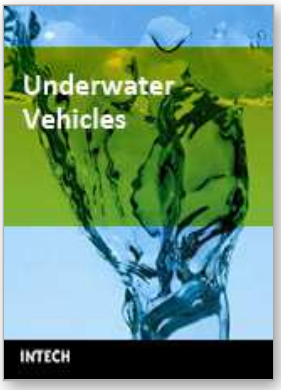

Underwater Vehicles

Edited by Alexander V. Inzartsev

ISBN 978-953-7619-49-7
Hard cover, 582 pages
Publisher InTech
Published online 01, January, 2009
Published in print edition January, 2009

For the latest twenty to thirty years, a significant number of AUVs has been created for the solving of wide spectrum of scientific and applied tasks of ocean development and research. For the short time period the AUVs have shown the efficiency at performance of complex search and inspection works and opened a number of new important applications. Initially the information about AUVs had mainly review-advertising character but now more attention is paid to practical achievements, problems and systems technologies. AUVs are losing their prototype status and have become a fully operational, reliable and effective tool and modern multi-purpose AUVs represent the new class of underwater robotic objects with inherent tasks and practical applications, particular features of technology, systems structure and functional properties.

InTech Europe
University Campus STeP Ri
Slavka Krautzeka 83/A
51000 Rijeka, Croatia
Phone: +385 (51) 770 447
Fax: +385 (51) 686 166
www.intechopen.com

InTech China
Unit 405, Office Block, Hotel Equatorial Shanghai
No.65, Yan An Road (West), Shanghai, 200040, China
中国上海市延安西路65号上海国际贵都大饭店办公楼405单元
Phone: +86-21-62489820
Fax: +86-21-62489821